

The contrarotational fluxionality of [3,3-(PMe₂Ph)₂-*clos*o-3,1,2-PtC₂B₉H₁₁] and related species

Supplementary information

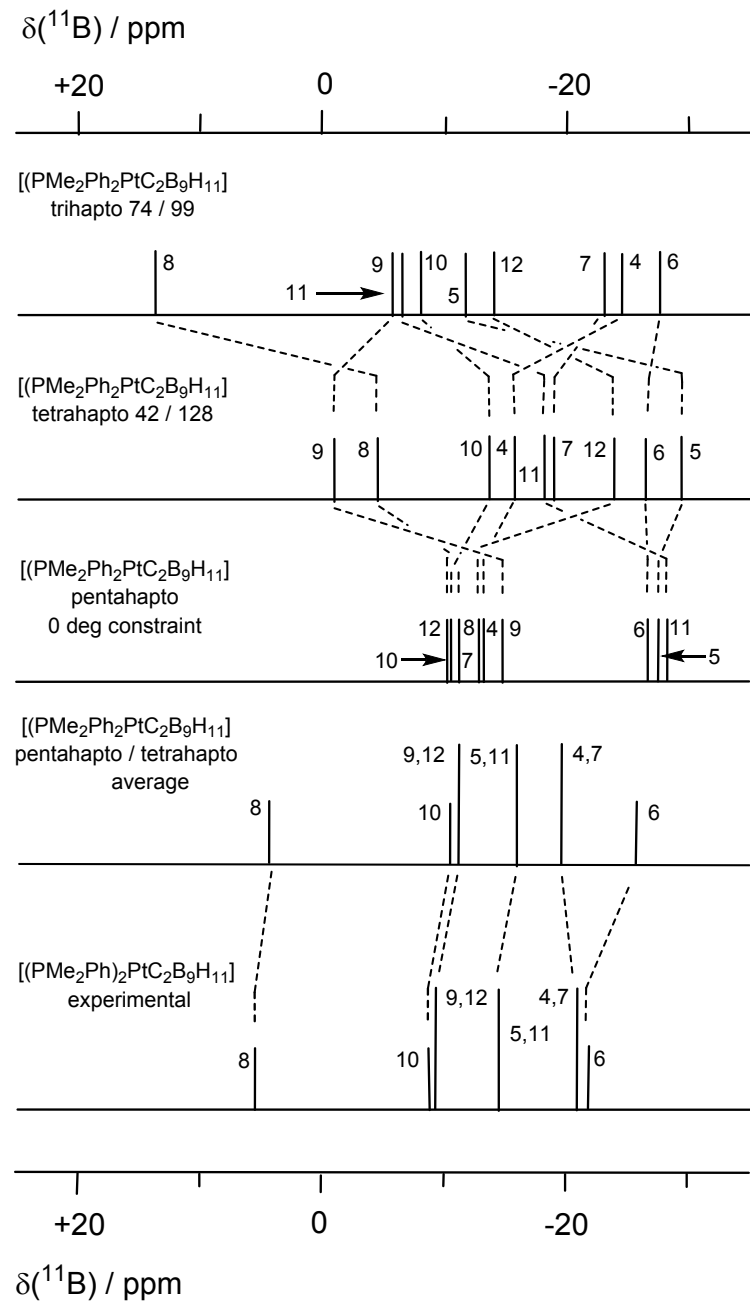
Robert D. Kennedy^{a,b} and John D. Kennedy^{b,c,*}

^a Department of Chemistry and Biochemistry, University of California, Los Angeles, California 90095-1569, USA; Department of Chemistry, Northwestern University, Evanston, Illinois, 60208, USA.

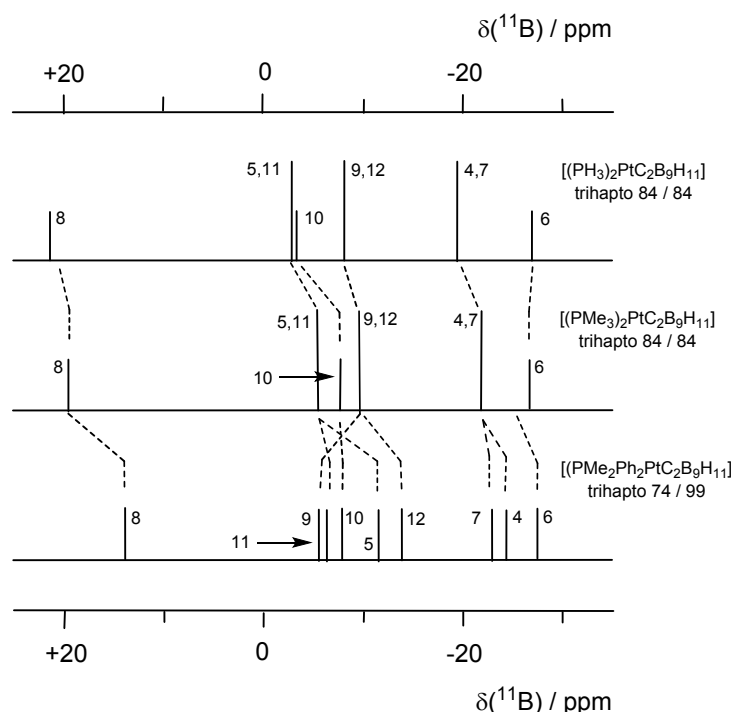
^b School of Chemistry, University of Leeds, Leeds, UK LS2 9JT.

^c Institute of Inorganic Chemistry, Academy of Sciences of the Czech Republic, 25068 Řež u Prahy, The Czech Republic

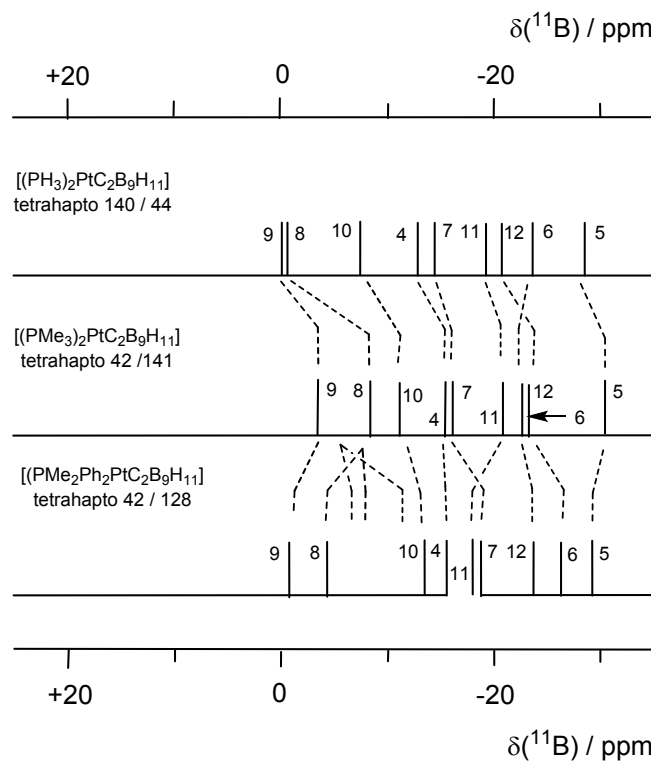
Supplementary plot S1. Representations of the boron nuclear magnetic shieldings, expressed as ^{11}B NMR chemical shifts $\delta(^{11}\text{B})$, and relative intensities, as calculated for the *trihapto*, *tetrahapto* and *pentahapto* conformations of $[(\text{PMe}_2\text{Ph})_2\text{PtC}_2\text{B}_9\text{H}_{11}]$ (upper three diagrams), the mean of the *trihapto* and *tetrahapto* values (fourth diagram), and the experimentally determined ^{11}B NMR chemical shift values $\delta(^{11}\text{B})$ for $[(\text{PMe}_2\text{Ph})_2\text{PtC}_2\text{B}_9\text{H}_{11}]$ (bottom diagram; data from reference 15).



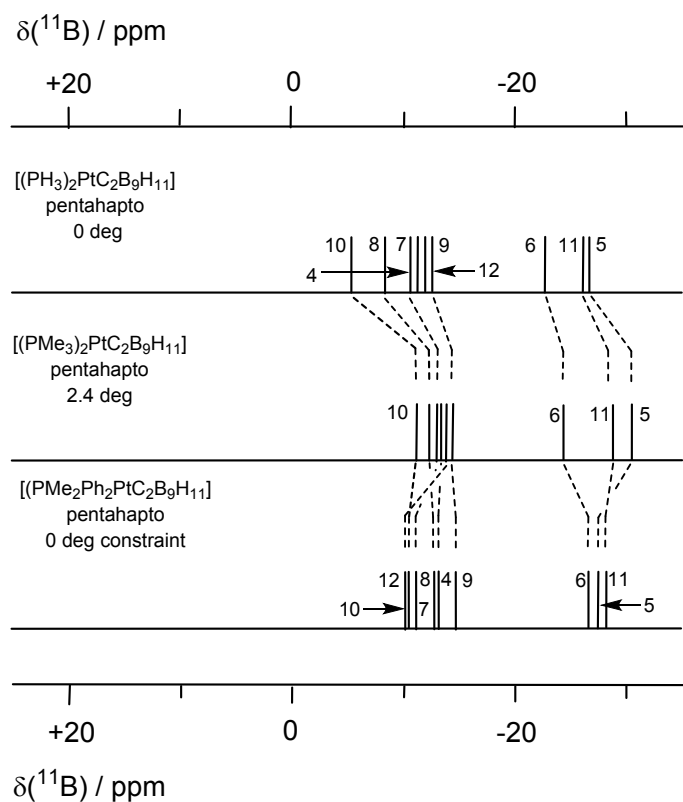
Supplementary plot S2. Representations of the boron nuclear magnetic shieldings, expressed as ^{11}B NMR chemical shifts $\delta(^{11}\text{B})$, and relative intensities, as calculated for the *trihapto* conformations of $[(\text{PH}_3)_2\text{PtC}_2\text{B}_9\text{H}_{11}]$ (top diagram) $[(\text{PMe}_3)_2\text{PtC}_2\text{B}_9\text{H}_{11}]$ (middle diagram) and $[(\text{PMe}_2\text{Ph})_2\text{PtC}_2\text{B}_9\text{H}_{11}]$ (lower diagram). Figure 6 in the text displays the same data, but with each of the (4,7), (5,11) and (9,12) pairs averaged and combined to reflect that they will be exchanging positions by libration across the notional $\text{Pt}(3)\text{B}(6)\text{B}(8)\text{B}(10)$ plane.



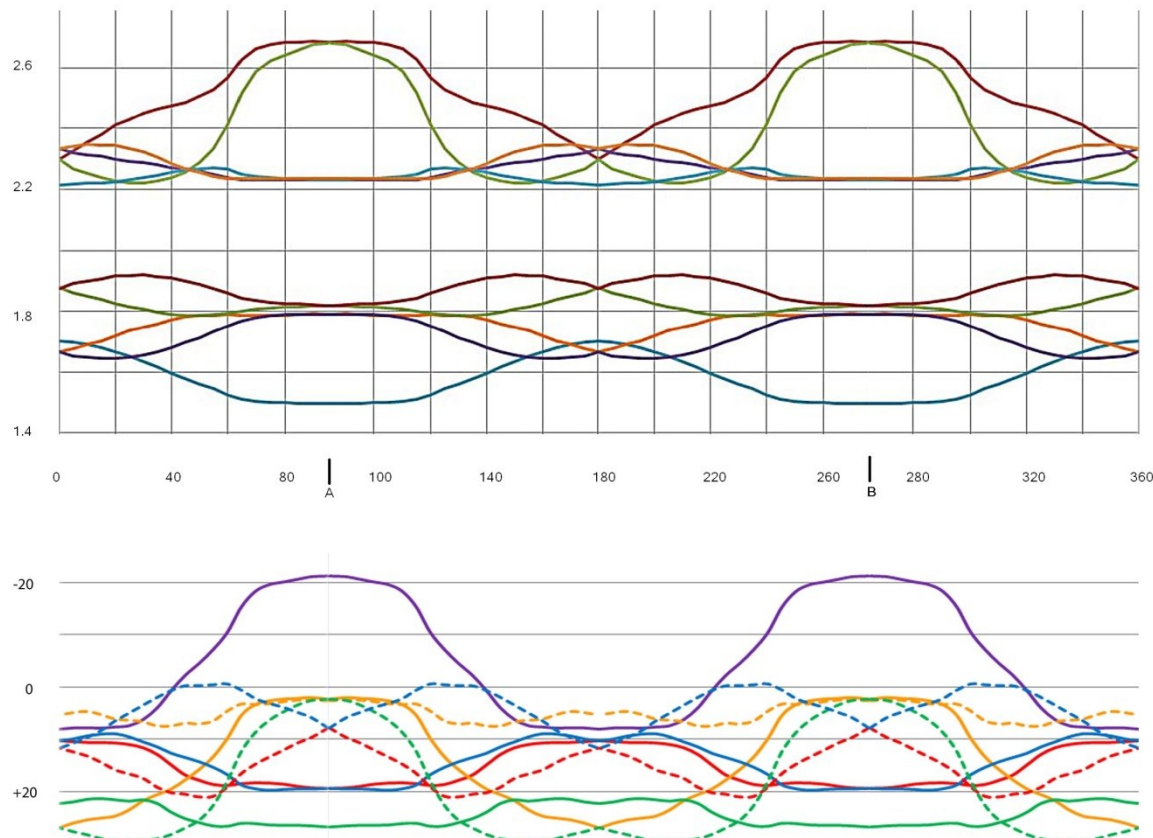
Supplementary plot S3. Representations of the boron nuclear magnetic shieldings, expressed as ^{11}B NMR chemical shifts $\delta(^{11}\text{B})$, and relative intensities, as calculated for the *tetrahapto* conformations of $[(\text{PH}_3)_2\text{PtC}_2\text{B}_9\text{H}_{11}]$ (top diagram) $[(\text{PMe}_3)_2\text{PtC}_2\text{B}_9\text{H}_{11}]$ (middle diagram) and $[(\text{PMe}_2\text{Ph})_2\text{PtC}_2\text{B}_9\text{H}_{11}]$ (lower diagram)



Supplementary plot S4. Representations of the boron nuclear magnetic shieldings, expressed as ^{11}B NMR chemical shifts $\delta(^{11}\text{B})$, and relative intensities, as calculated for the *pentahapto* conformations of $[(\text{PH}_3)_2\text{PtC}_2\text{B}_9\text{H}_{11}]$ (top diagram) $[(\text{PMe}_3)_2\text{PtC}_2\text{B}_9\text{H}_{11}]$ (middle diagram) and $[(\text{PMe}_2\text{Ph})_2\text{PtC}_2\text{B}_9\text{H}_{11}]$ (lower diagram)



Supplementary Figure S5. A representation to illustrate the general overall 360° rotational behaviour of calculated parameters for the model compound [3,3-(PH₃)₂-*clos*o-3,1,2-PtC₂B₉H₁₁]. Upper diagram: interatomic distances in Å. Lower diagram: boron nuclear shieldings as $\delta(^{11}\text{B})/\text{ppm}$. The curves are derived from combinations of the diagrams in Figure 5 and Figure 8 in the main text and their mirrorings. There are C1/C2, B4/B7, B5/B12 and B9/B11 coincidences at the 0° and 180 ° points, and at the notional 90° and 120° points **A** and **B**. Because of the nature of the calculational incrementation based on the dihedral angle, and because there is cluster flexing, and in addition the dihedral angle does not map directly onto the simplistic projection angle θ of schematic structure **XI**, the defining quarter-rotation occurs over 84°. In this particular representation, therefore, there is an effective 12° ‘compression’ around the notional 90 ° and 270 ° points **A** and **B**.



Supplementary Table 1. Comparisons of calculated structures of $[\text{Pt}(\text{C}_2\text{B}_9\text{H}_{11})(\text{PH}_3)_2]$ (global minimum), $[\text{Pt}(\text{C}_2\text{B}_9\text{H}_{11})(\text{PMMe}_3)_2]$ (global minimum), and $[\text{Pt}(\text{C}_2\text{B}_9\text{H}_{11})(\text{PPhMe}_2)_2]$ (global minimum) with the crystal structures of $[\text{Pt}(\text{C}_2\text{B}_9\text{H}_{11})(\text{PEt}_3)_2]$ and $[\text{Pt}(\text{C}_2\text{B}_9\text{H}_{11})(\text{PPhMe}_2)_2]$ (75° conformer). Distances (Å), angles (deg) and torsions (deg).

| | Calc 84/84 ($\text{PH}_3)_2$) | Calc 84/84 ($\text{PMMe}_3)_2$) | Calc 74/99 ($\text{PPhMe}_2)_2$) | JDK 75/99 ($\text{PPhMe}_2)_2$) | Mogos 67/96 ($\text{PEt}_3)_2$) |
|------------|------------------------------------|--------------------------------------|---------------------------------------|--------------------------------------|--------------------------------------|
| Dihedral 1 | 84.102 | 84.469 | 73.786 | 74.90(47) | 66.89(2) |
| Dihedral 2 | 84.053 | 84.393 | 98.788 | 98.95(45) | 95.66(2) |
| Pt(3)–C(1) | 2.684 | 2.705 | 2.612 | 2.529(7) | 2.529(16) |
| Pt(3)–C(2) | 2.684 | 2.705 | 2.674 | 2.574(7) | 2.612(52) |
| Pt(3)–B(4) | 2.235 | 2.265 | 2.254 | 2.266(8) | 2.282(30) |
| Pt(3)–B(7) | 2.235 | 2.265 | 2.268 | 2.260(7) | 2.278(40) |
| Pt(3)–B(8) | 2.232 | 2.235 | 2.249 | 2.269(49) | 2.264(15) |
| C(1)–C(2) | 1.496 | 1.499 | 1.506 | 1.495(10) | 1.529(30) |
| C(2)–B(7) | 1.791 | 1.764 | 1.754 | 1.712(11) | 1.742(2) |
| B(7)–B(8) | 1.819 | 1.812 | 1.818 | 1.804(12) | 1.809(24) |
| B(8)–B(4) | 1.819 | 1.812 | 1.803 | 1.783(12) | 1.803(20) |
| B(4)–C(1) | 1.791 | 1.764 | 1.769 | 1.746(17) | 1.755(2) |
| Pt(3)–P(A) | 2.277 | 2.294 | 2.310 | 2.260(2) | 2.284(27) |
| Pt(3)–P(B) | 2.277 | 2.294 | 2.286 | 2.271(2) | 2.275(46) |
| P–Pt–P | 100.799 | 104.493 | 95.261 | 92.33(6) | 98.36(1) |

Supplementary Table 2. Comparisons of calculated structures of $[\text{Pt}(\text{C}_2\text{B}_9\text{H}_{11})(\text{PH}_3)_2]$ (dihedral constrained to 42.5°), $[\text{Pt}(\text{C}_2\text{B}_9\text{H}_{11})(\text{PH}_3)_2]$ (dihedral constrained to 130° [mirror imaged for comparison]), $[\text{Pt}(\text{C}_2\text{B}_9\text{H}_{11})(\text{PMMe}_3)_2]$ (secondary minimum, no constraints) $[\text{Pt}(\text{C}_2\text{B}_9\text{H}_{11})(\text{PPhMe}_2)_2]$ (41° constrained from crystal structure) with the crystal structure of $[\text{Pt}(\text{C}_2\text{B}_9\text{H}_{11})(\text{PPhMe}_2)_2]$ (41° conformer). Distances (Å), angles (deg) and torsions (deg).

| | Calc 43/127 ($\text{PH}_3)_2$) | Calc 130/55 ($\text{PH}_3)_2$ mirror) | Calc 42/141 ($\text{PMMe}_3)_2$) | Calc 52/124 ($\text{PPhMe}_2)_2$) | Calc 42/128 ($\text{PPhMe}_2)_2$) | exp JDK 41/129 ($\text{PPhMe}_2)_2$) |
|------------|-------------------------------------|---|---------------------------------------|--|--|---|
| Dihedral 1 | 42.5 | 54.593 | 42.006 | 51.889 | 41.647 | 41.65(52) |
| Dihedral 2 | 126.518 | 130.00 | 141.266 | 124.061 | 127.622 | 129.38(43) |
| Pt(3)–C(1) | 2.292 | 2.289 | 2.274 | 2.331 | 2.327 | 2.303(7) |
| Pt(3)–C(2) | 2.520 | 2.507 | 2.532 | 2.551 | 2.553 | 2.515(7) |
| Pt(3)–B(4) | 2.259 | 2.259 | 2.275 | 2.269 | 2.278 | 2.283(9) |
| Pt(3)–B(7) | 2.269 | 2.255 | 2.326 | 2.282 | 2.294 | 2.307(7) |
| Pt(3)–B(8) | 2.257 | 2.268 | 2.257 | 2.265 | 2.258 | 2.265(7) |
| C(1)–C(2) | 1.564 | 1.561 | 1.586 | 1.553 | 1.563 | 1.570(10) |
| C(2)–B(7) | 1.704 | 1.712 | 1.664 | 1.696 | 1.689 | 1.668(11) |
| B(7)–B(8) | 1.892 | 1.890 | 1.890 | 1.871 | 1.876 | 1.826(10) |
| B(8)–B(4) | 1.789 | 1.785 | 1.798 | 1.792 | 1.790 | 1.788(12) |
| B(4)–C(1) | 1.780 | 1.787 | 1.750 | 1.758 | 1.750 | 1.737(12) |
| Pt(3)–P(A) | 2.297 | 2.294 | 2.310 | 2.313 | 2.317 | 2.288(2) |
| Pt(3)–P(B) | 2.243 | 2.243 | 2.261 | 2.267 | 2.264 | 2.235(2) |
| P–Pt–P | 96.809 | 96.912 | 97.799 | 95.964 | 95.111 | 93.11(6) |

Supplementary Table 3. NMR chemical shifts for $[\text{Pt}(\text{C}_2\text{B}_9\text{H}_{11})(\text{PH}_3)_2]$, $[\text{Pt}(\text{C}_2\text{B}_9\text{H}_{11})(\text{PMe}_3)_2]$ and $[\text{Pt}(\text{C}_2\text{B}_9\text{H}_{11})(\text{PPhMe}_2)_2]$. The shifts are presented relative to D_{2h} B_2H_6 [PBE1PBE 6-311+G(2d,p), optimized at the PBE1PBE/6-31G(d) level] which has a calculated shielding tensor of 86.5889, converted to 16.6 ppm vs $\text{BF}_3 \cdot \text{OEt}_2$. The values in the $(\text{PH}_3)_2$ column were obtained from a mirror-image of the original calculation for comparative purposes *i.e.* the dihedral was constrained to 140°. Catch my drift?

| | $(\text{PH}_3)_2$ 84/84 | $(\text{PMe}_3)_2$ 84/84 | $(\text{PPhMe}_2)_2$ 74/99 | $(\text{PH}_3)_2$ 140/44 | $(\text{PMe}_3)_2$ 42/141 | $(\text{PPhMe}_2)_2$ 42/128 | experimental NMR data |
|-------|----------------------------|-----------------------------|-------------------------------|-----------------------------|------------------------------|--------------------------------|--------------------------|
| C(1) | 67.8171 | 62.8406 | 61.3264 | 42.6277 | 39.0519 | 46.0702 | |
| C(2) | 67.8403 | 62.8605 | 55.6402 | 40.1228 | 35.9277 | 37.6189 | |
| B(4) | -19.3326 | -22.8671 | -23.5011 | -12.6254 | -15.3748 | -15.8695 | |
| B(5) | -2.3080 | -5.2104 | -11.5289 | -28.1213 | -30.5719 | -28.7001 | |
| B(6) | -26.6930 | -26.9458 | -27.5828 | -23.8858 | -22.5786 | -23.8244 | |
| B(7) | -19.3232 | -22.8744 | -21.6836 | -14.8701 | -16.4550 | -18.3725 | |
| B(8) | 21.1992 | 19.1140 | 14.3727 | -0.6672 | -8.4806 | -4.1542 | |
| B(9) | -7.8053 | -9.7095 | -5.1479 | -0.6514 | -3.6759 | -0.6842 | |
| B(10) | -2.5705 | -7.8423 | -7.7864 | -7.4206 | -11.5733 | -13.0359 | |
| B(11) | -2.3078 | -5.2182 | -5.4953 | -19.4407 | -20.3478 | -18.1216 | |
| B(12) | -7.7813 | -9.6772 | -14.6894 | -20.172 | -22.6017 | -23.8976 | |

Supplementary Table 4. NMR chemical shifts for $[\text{Pt}(\text{C}_2\text{B}_9\text{H}_{11})(\text{PH}_3)_2]$, $[\text{Pt}(\text{C}_2\text{B}_9\text{H}_{11})(\text{PMe}_3)_2]$ and $[\text{Pt}(\text{C}_2\text{B}_9\text{H}_{11})(\text{PPhMe}_2)_2]$. The shifts are presented relative to D_{2h} B_2H_6 [PBE1PBE 6-311+G(2d,p), optimized at the PBE1PBE/6-31G(d) level] which has a calculated shielding tensor of 86.5889, converted to 16.6 ppm vs $\text{BF}_3 \cdot \text{OEt}_2$. “TS” for the last column is not a verified TS but a constrained ‘perpendicular’ optimization (0 deg)

| | $(\text{PH}_3)_2$ TS | $(\text{PMe}_3)_2$ TS | $(\text{PPhMe}_2)_2$ “TS” |
|-------|-------------------------|--------------------------|------------------------------|
| C(1) | 43.0148 | 35.785 | 37.8550 |
| C(2) | 43.0025 | 35.9483 | 35.4377 |
| B(4) | -10.2653 | -12.4723 | -13.7168 |
| B(5) | -26.8662 | -28.6766 | -27.3464 |
| B(6) | -22.2061 | -24.32 | -23.7567 |
| B(7) | -10.2618 | -12.8585 | -11.5123 |
| B(8) | -8.0174 | -11.9065 | -13.0364 |
| B(9) | -11.6435 | -13.2254 | -14.7923 |
| B(10) | -5.3207 | -10.7927 | -10.5579 |
| B(11) | -26.8602 | -28.0336 | -28.0498 |
| B(12) | -11.6435 | -13.6861 | -10.2064 |

Supplementary Table 5. $[(\text{PMe}_3)_2\text{PtC}_2\text{B}_9\text{H}_{11}]$ nuclear magnetic shielding calculations

opt/freq/minimum at 84.47 deg

| | | ref | corr | final |
|-----|----------|----------|------|-----------------|
| C1 | 124.4908 | 187.3314 | 0 | 62.8406 |
| C2 | 124.4709 | 187.3314 | 0 | 62.8605 |
| Pt3 | 94.2083 | | | |
| B4 | 126.056 | 86.5889 | 16.6 | -22.8671 |

| | | | | |
|-----|----------|---------|------|-----------------|
| B5 | 108.3993 | 86.5889 | 16.6 | -5.2104 |
| B6 | 130.1347 | 86.5889 | 16.6 | -26.9458 |
| B7 | 126.0633 | 86.5889 | 16.6 | -22.8744 |
| B8 | 84.0749 | 86.5889 | 16.6 | 19.114 |
| B9 | 112.8984 | 86.5889 | 16.6 | -9.7095 |
| B10 | 111.0312 | 86.5889 | 16.6 | -7.8423 |
| B11 | 108.4071 | 86.5889 | 16.6 | -5.2182 |
| B12 | 112.8661 | 86.5889 | 16.6 | -9.6772 |
| P25 | 317.4401 | 582.563 | -266 | -0.8771 |
| P24 | 317.4015 | 582.563 | -266 | -0.8385 |

Higher minimum at 42.01 deg

| | | ref | corr | final |
|-----|----------|----------|------|-----------------|
| C1 | 148.2795 | 187.3314 | 0 | 39.0519 |
| C2 | 151.4037 | 187.3314 | 0 | 35.9277 |
| Pt3 | 88.3219 | | | |
| B4 | 118.5637 | 86.5889 | 16.6 | -15.3748 |
| B5 | 133.7608 | 86.5889 | 16.6 | -30.5719 |
| B6 | 125.7675 | 86.5889 | 16.6 | -22.5786 |
| B7 | 119.6439 | 86.5889 | 16.6 | -16.455 |
| B8 | 111.6695 | 86.5889 | 16.6 | -8.4806 |
| B9 | 106.8648 | 86.5889 | 16.6 | -3.6759 |
| B10 | 114.7622 | 86.5889 | 16.6 | -11.5733 |
| B11 | 123.5367 | 86.5889 | 16.6 | -20.3478 |
| B12 | 125.7906 | 86.5889 | 16.6 | -22.6017 |
| P25 | 293.7617 | 582.563 | -266 | 22.8013 |
| P24 | 339.7368 | 582.563 | -266 | -23.1738 |

Transition state at 2.4 deg

| | | ref | corr | final |
|-----|----------|----------|------|-----------------|
| C1 | 151.5464 | 187.3314 | 0 | 35.785 |
| C2 | 151.3831 | 187.3314 | 0 | 35.9483 |
| Pt3 | 91.7402 | | | |
| B4 | 115.6612 | 86.5889 | 16.6 | -12.4723 |
| B5 | 131.8655 | 86.5889 | 16.6 | -28.6766 |
| B6 | 127.5089 | 86.5889 | 16.6 | -24.32 |
| B7 | 116.0474 | 86.5889 | 16.6 | -12.8585 |
| B8 | 115.0954 | 86.5889 | 16.6 | -11.9065 |
| B9 | 116.4143 | 86.5889 | 16.6 | -13.2254 |
| B10 | 113.9816 | 86.5889 | 16.6 | -10.7927 |
| B11 | 131.2225 | 86.5889 | 16.6 | -28.0336 |
| B12 | 116.875 | 86.5889 | 16.6 | -13.6861 |
| P13 | 340.4051 | 582.563 | -266 | -23.8421 |
| P14 | 279.7969 | 582.563 | -266 | 36.7661 |

Supplementary Table 6. $[(\text{PMe}_2\text{Ph})_2\text{PtC}_2\text{B}_9\text{H}_{11}]$ nuclear magnetic shielding calculations

full optimization starting from X-ray result: ‘parallel’ conformation

| | | ref | corr | final |
|-----|----------|----------|---------|-----------------|
| C1 | 126.0050 | 187.3314 | 0.0000 | +61.3264 |
| C2 | 131.6912 | 187.3314 | 0.0000 | +55.6402 |
| Pt3 | 96.6839 | | | |
| B4 | 126.6900 | 86.5889 | 16.6000 | -23.5011 |
| B5 | 114.7178 | 86.5889 | 16.6000 | -11.5289 |
| B6 | 130.7717 | 86.5889 | 16.6000 | -27.5828 |
| B7 | 124.8725 | 86.5889 | 16.6000 | -21.6836 |
| B8 | 88.8162 | 86.5889 | 16.6000 | +14.3727 |

| | | | | |
|-----|----------|----------|-----------|-----------------|
| B9 | 108.3368 | 86.5889 | 16.6000 | -5.1479 |
| B10 | 110.9753 | 86.5889 | 16.6000 | -7.7864 |
| B11 | 108.6842 | 86.5889 | 16.6000 | -5.4953 |
| B12 | 117.8783 | 86.5889 | 16.6000 | -14.6894 |
| P13 | 302.8393 | 582.5630 | -266.0000 | +13.7237 |
| P14 | 313.0859 | 582.5630 | -266.0000 | +3.4771 |

PMe₂Ph starting from X-ray result, one angle constr. 41.647 deg: ‘diagonal’ conformation

| | | ref | corr | final |
|-----|----------|----------|-----------|-----------------|
| C1 | 141.2611 | 187.3314 | 0.0000 | +46.0703 |
| C2 | 149.7125 | 187.3314 | 0.0000 | +37.6189 |
| Pt3 | 94.1103 | | | |
| B4 | 119.0584 | 86.5889 | 16.6000 | -15.8695 |
| B5 | 131.8890 | 86.5889 | 16.6000 | -28.7001 |
| B6 | 127.0133 | 86.5889 | 16.6000 | -23.8244 |
| B7 | 121.5614 | 86.5889 | 16.6000 | -18.3725 |
| B8 | 107.3431 | 86.5889 | 16.6000 | -4.1542 |
| B9 | 103.8731 | 86.5889 | 16.6000 | -0.6842 |
| B10 | 116.2248 | 86.5889 | 16.6000 | -13.0359 |
| B11 | 121.3105 | 86.5889 | 16.6000 | -18.1216 |
| B12 | 127.0865 | 86.5889 | 16.6000 | -23.8976 |
| P1 | 323.6159 | 582.5630 | -266.0000 | -7.0529 |
| P2 | 280.0446 | 582.5630 | -266.0000 | +36.5184 |

angle constrained to 0 deg; ‘perpendicular’ conformation

| | | ref | corr | final |
|-----|----------|----------|-----------|-----------------|
| C1 | 149.4764 | 187.3314 | 0.0000 | +37.8550 |
| C2 | 151.8937 | 187.3314 | 0.0000 | +35.4377 |
| Pt3 | 96.5043 | | | |
| B4 | 116.9057 | 86.5889 | 16.6000 | -13.7168 |
| B5 | 130.5353 | 86.5889 | 16.6000 | -27.3464 |
| B6 | 126.9456 | 86.5889 | 16.6000 | -23.7567 |
| B7 | 114.7012 | 86.5889 | 16.6000 | -11.5123 |
| B8 | 116.2253 | 86.5889 | 16.6000 | -13.0364 |
| B9 | 117.9812 | 86.5889 | 16.6000 | -14.7923 |
| B10 | 113.7468 | 86.5889 | 16.6000 | -10.5579 |
| B11 | 131.2387 | 86.5889 | 16.6000 | -28.0498 |
| B12 | 113.3953 | 86.5889 | 16.6000 | -10.2064 |
| P1 | 329.5430 | 582.5630 | -266.0000 | -12.9800 |
| P2 | 269.0471 | 582.5630 | -266.0000 | +47.5159 |

Supplementary citation information (reference XX)

Gaussian 03, Revision B.04, Frisch, M. J.; Trucks, G. W.; Schlegel, H. B.; Scuseria, G. E.; Robb, M. A.; Cheeseman, J. R.; Montgomery, Jr., J. A.; Vreven, T.; Kudin, K. N.; Burant, J. C.; Millam, J. M.; Iyengar, S. S.; Tomasi, J.; Barone, V.; Mennucci, B.; Cossi, M.; Scalmani, G.; Rega, N.; Petersson, G. A.; Nakatsuji, H.; Hada, M.; Ehara, M.; Toyota, K.; Fukuda, R.; Hasegawa, J.; Ishida, M.; Nakajima, T.; Honda, Y.; Kitao, O.; Nakai, H.; Klene, M.; Li, X.; Knox, J. E.; Hratchian, H. P.; Cross, J. B.; Bakken, V.; Adamo, C.; Jaramillo, J.; Gomperts, R.; Stratmann, R. E.; Yazyev, O.; Austin, A. J.; Cammi, R.; Pomelli, C.; Ochterski, J. W.; Ayala, P. Y.; Morokuma, K.; Voth, G. A.; Salvador, P.; Dannenberg, J. J.; Zakrzewski, V. G.; Dapprich, S.; Daniels, A. D.; Strain, M. C.; Farkas, O.; Malick, D. K.; Rabuck, A. D.; Raghavachari, K.; Foresman, J. B.; Ortiz, J. V.; Cui, Q.; Baboul, A. G.; Clifford, S.; Cioslowski, J.; Stefanov, B. B.; Liu, G.; Liashenko, A.; Piskorz, P.; Komaromi,

I.; Martin, R. L.; Fox, D. J.; Keith, T.; Al-Laham, M. A.; Peng, C. Y.; Nanayakkara, A.; Challacombe, M.; Gill, P. M. W.; Johnson, B.; Chen, W.; Wong, M. W.; Gonzalez, C.; and Pople, J. A.; *Gaussian, Inc., Wallingford CT*, 2004.